Carbohydrate Polymers 99 (2014) 608–616

Contents lists available at ScienceDirect

Carbohydrate Polymers

journal homepage: www.elsevier.com/locate/carbpol

Preparation of microcapsules by complex coacervation of gum Arabic and chitosan

Chloé Butstraen[a,b], Fabien Salaün[a,b,*]

[a] Univ Lille Nord de France, F-59000 Lille, France
[b] ENSAIT, GEMTEX, F-59100 Roubaix, France

ARTICLE INFO

Article history:
Received 18 December 2012
Received in revised form 26 August 2013
Accepted 4 September 2013
Available online 8 September 2013

Keywords:
Microcapsules
Oil in water emulsion
Chitosan
Gum Arabic
Tripolyphosphate
Complex coacervation

ABSTRACT

Gum Arabic–chitosan microcapsules containing a commercially available blend of triglycerides (Miglyol 812 N) as core phase were synthesized by complex coacervation. This study was conducted to clarify the influence of different parameters on the encapsulation process, i.e. during the emulsion formation steps and during the shell formation, using conductometry, zeta potential, surface and interface tension measurement and Fourier-transform infrared spectroscopy. By carefully analyzing the influencing factors including phase volume ratio, stirring rate and time, pH, reaction time, biopolymer ratio and crosslinking effect, the optimum synthetic conditions were found out. For the emulsion step, the optimum phase volume ratio chosen was 0.10 and an emulsion time of 15 min at 11,000 rpm was selected. The results also indicated that the optimum formation of these complexes appears at a pH value of 3.6 and a weight ratio of chitosan to gum Arabic mixtures of 0.25.

1. Introduction

Microencapsulation was early studied in 1929 by Bungenberg de Jong & Kruyt to prepare gelatin sphere by coacervation (Bungenberg de Jong & Kruyt, 1929), and by Barret Green for the development of the first carbon-free carbon paper in the world in the fifties. This process consists in coating tiny droplets or particles of an active substance such as drugs, proteins, hormones, pesticides, fertilizers, cosmetics, perfumes or dyes with a thin barrier wall to obtain individualized microparticles. The main purposes of this technology are the stabilization of particles, the protection and/or isolation of active core material from surroundings which allows materials to be handled more easily for application. Thus, the advantages of microencapsulation are described as the controlled release of encapsulated bioactive materials, protection of encapsulated materials from oxidation, and imparting stability to environmental stress (Bansode, Banarjee, Gaikwad, Jadhav, & Thorat, 2010). Furthermore, the purpose of the microencapsulation is related to the particle permeability (Boh & Sumiga, 2008). The shell barrier involves natural or synthetic polymers as a continuous protective film to entrap the liquid or solid core material. Although textile applications of microencapsulation have been considered two decades later, a large range of uses, from fire resistant to medical textiles can be described nowadays (Nelson, 2002). The encapsulation step allows to manufacture textiles containing microcapsules by various ways to fix them within the fiber structure permanently, to embed them into a binder or to mix them into foam (Bendkowska, 2006; Salaün, Creach, Rault, & Almeras, 2013; Salaün, Devaux, Bourbigot, & Rumeau, 2010).

The functional performance of the microcapsules depends on the morphology, the chemical nature and the surface characteristics of the polymeric shell influenced by the process parameters (Yadav, Suresh, & Khilar, 1990). The choice of a particular process is determined by the solubility characteristics of the active compound and the shell material depending on the final use. Bioresourceable polymeric matrix, such as chitosan, has been already used to encapsulate active substance in the pharmaceutical industry due to its lack of toxicity, film forming capacity, high mucoadhesivity and tensile strength (Alonso, Gimeno, Sepúlveda-Sánchez, & Shirai, 2010; Garud & Garud, 2010; Pedro, Cabral-Albuquerque, Ferreira, & Sarmento, 2009). Chitosan microcapsules can be prepared by various approaches, i.e. simple coacervation or ionic gelation (Hsieh, Chang, & Gao, 2006), complex coacervation (de Kruif, Weinbreck, & de Vries, 2004), and layer-by-layer self-assembly technique (Chatterjee, Salaün, Campagne, Vaupre, & Beirão, 2012; Shao et al., 2009). In these microencapsulation processes, which are based on coacervation from an oil in water emulsion, the emulsion containing an anionic emulsifier is added to an aqueous chitosan solution before being converted into microcapsules by the addition of a suitable electrolyte such as alginate (Chávarri et al., 2010; Wu et al., 2009), gelatin (Hussain & Maji, 2008; Yuan et al.,

* Corresponding author at: ENSAIT-GEMTEX, 2 allée Louise et Victor Champier, BP 30329, 59056 Roubaix, France. Tel.: +33 3 20 25 64 59; fax: +33 3 20 27 25 97.
E-mail address: fabien.salaun@ensait.fr (F. Salaün).

0144-8617/$ – see front matter © 2013 Elsevier Ltd. All rights reserved.
http://dx.doi.org/10.1016/j.carbpol.2013.09.006

2007), silk fibroin (Deveci & Basal, 2009), carboxymetylcellulose (Gómez-Burgaz, García-Ochoa, & Torrado-Santiago, 2008), sodium lignosulfate or sulfate, and changing the pH. In addition, new complex coacervation systems based on chitosan have emerged these last years, i.e. α-lactabumin and β-lactoglobulin-chitosan (Lee & Hong, 2009), soy globulin-chitosan, pea and soybean protein isolate-chitosan (Elmer, Karaca, Low, & Nickerson, 2011; Huang, Sun, Xiao, & Yang, 2012), xanthan-chitosan (Argin-Soysal, Kofinas, & Lo, 2009), and gum Arabic–chitosan (Avadi et al., 2010; Coelho et al., 2011; Espinosa-Andrews, Sandoval-Castilla, Vázquez-Torres, Vernon-Carter, & Lobato-Calleros, 2010; Moschakis, Murray, & Biliaderis, 2010).

To increase the thermo-mechanical properties of the microcapsules, these hydrophilic polymers need to be cross-linked. Nevertheless, most of the chemical cross-linkers cited in the literature, such as formaldehyde, glutaraldehyde, glyoxal, diisocyanate, epichlorohydrin (Kumbar, Kulkarnu & Aminabhavi, 2002) have to be limited due to their toxicity, or also removed by washing with a suitable solvent to reach the biological acceptance. To overcome the restriction in using toxic crosslinkers, some studies propose genipin (Hussain & Maji, 2008; Yuan et al., 2007) as potential crosslinker as well as sodium tripolyphosphate (NaTPP) which is a non-toxic multivalent anion (Fernandes, de Oliveira, Fatibello-Filho, Spinelli, & Vieira, 2008; Li & Huang, 2012; Mi, Shyu, Lee, & Wong, 1999; Morris, Castile, Smith, Adams, & Harding, 2011). Tripolyphosphate is a polyanion ($P_3O_{10}^{5-}$), and can interact with positively charged amino groups ($-NH_3^+$) of chitosan by electrostatic forces to form intermolecular ionic linkages or crosslinked networks.

The present study aimed to develop and characterize chitosan–gum Arabic coacervate microcapsules strengthened by the NaTPP induced crosslinking process. This work is composed of the following three phases, i.e. firstly, the key factors influencing the emulsion step; secondly, the formation of the coacervated particles and finally the introduction of the crosslinker. Thus, a two step microencapsulation process has been studied. The first step is the liquid-liquid dispersion of the active substance in the continuous phase and the second step is the microencapsulation carried out by complex coacervation. The dispersion of the active substance, an oily colored phase, in the continuous phase is the determining step in establishing the size distribution of the final microcapsules. This step is affected to a great extent by the physicochemical properties of the two immiscible phases as well as by the characteristics of the agitation system. Variations in these physical and design parameters influence the size distribution of the dispersed organic phase. Furthermore, the complex coacervation, taken place between charged biopolymers, is mainly affected by pH, ionic strength, biopolymer ratio as well as the mobility of the macromolecular chains and their charge density. Thus, to control the morphology and to prepare the microcapsules having the desired physical properties, it is necessary to determine the coacervation mechanism. In this study, experiments were conducted to characterize the influence of parameters governing the emulsion step, and since the complex coacervation between chitosan and gum Arabic is few reported in the literature, the purpose of this research is to explore the mechanism based on a thermodynamical approach and to investigate the effect of biopolymer ratio and cross-linker amount on the microcapsules properties using Fourier transform infrared spectroscopy (FTIR), and scanning electron microscopy (SEM).

2. Materials and methods

2.1. Materials

Low molecular weight chitosan (Chi) (deacetylation degree = 75–85% and molecular weight = 50,000–190,000), gum Arabic (GA) (molecular weight = 250,000 approx.), and sodium tripolyphosphate (NaTPP) were purchased from Sigma–Aldrich Co. LLC, and were selected as shell materials. The core material is composed of an oil soluble Red dye purchased from Bayer dispersed in Miglyol 812 N (Sasol, France). All other analytical grade chemicals such as sodium hydroxide (NaOH), acetic acid, hydrochloric acid (HCl) were purchased from Sigma–Aldrich Co.

2.2. Preparation of microcapsules

2.2.1. Solutions preparation

All chitosan solutions were prepared in acetic acid solution (2%, v/v). Chi solutions (1, 2 or 3%, w/v, pH 4) were prepared by completely dissolving 1, 2 or 3.0 g of low molecular weight CS powder in 100 ml aqueous solution of 2% (v/v) acetic acid under magnetic stirring condition (1000 rpm) at 45 °C. Gum Arabic solutions (1, 2, 3, 5, 8 or 10%, w/v, pH 4.5–5) were prepared by dispersing the required amount of gum Arabic powder in 100 ml of de-ionized water. Tripolyphosphate solution was prepared by dissolution of 2.0 g of sodium tripolyphosphate in 100 ml of de-ionized water. The pH value of NaTPP solutions was adjusted from original (pH ~8) to pH 3.6 using acetic acid (2%, v/v). Miglyol solution, used as core formulation, was prepared by dissolution of 50 mg of Red dye in 100 ml of Miglyol 812 at 50 °C under magnetic stirring condition (1000 rpm).

2.2.2. Microcapsule formation

Miglyol solution (5, 10, 15 or 20 ml) was added into 100 ml of an aqueous solution of gum Arabic (pH 3.6). This mixture was vigorously dispersed by a homogenizer (ultra turrax high speed homogenizer (Ika T 25 basic, Germany)) at room temperature at 11,000 rpm during 5, 10, 15, 20, 25 or 30 min to create an oil in water emulsion. GA-Chi coacervation was obtained by the dropwise addition of chitosan solution (pH 3.6) in the needed proportions, estimated on the basis of the equivalence point between them to obtain charge neutralization of the functional groups. NaTPP was then adding to crosslink the formed particles, the solution were left at 1000 rpm during 2 h. Afterwards the resulted microcapsules were separated by decantation.

2.3. Analytical methods

2.3.1. Tensiometry

Surface tensions of the various liquids and the interfacial tension between each liquid phase were performed at 20 °C by the Wilhelmy's method using Prolabo TD2000 tensiometer according to the ASTM D971, or by contact angle measurements using GBX Digidrop Contact Angle meter by sessile drop technique for the coacervates. The vessel was washed with detergent, placed in chromosulfuric acid overnight, washed with distilled water, and briefly flamed with a Bunsen burner prior to use. The platinum plate was rinsed in acetone and distilled water, and flamed before use. The accuracy of measurement was ±0.1 mN/m. The measurements were pentaplicated and the mean values were considered for analysis.

The contact angles were estimated with a goniometer equipped with a special optical system and a camera. A droplet of test liquid (6 μl) was deposited on the substrate to study, and the image was analyzed to determine the contact angle between the liquid and the solid. The surface tension (γ) of the materials was obtained from a combination of the dispersion (γ^d) and polar (γ^p) components of the surface tension. The two test liquids used to determine the characteristics of the coacervated particles were water (γ = 72.8 mN/m, γ^d = 21.8 mN/m, γ^p = 51.0 mN/m) and methylene iodide (γ = 50.8 mN/m, γ^d = 48.5 mN/m, γ^p = 2.3 mN/m). Interfacial tensions between the coacervated microparticles and

the various liquids (e.g. continuous phase and miglyol) were determined by measuring the contact angle (θ) of each liquid against the particles. At least five measurements were made with each liquid and the mean contact angle was used to calculate the solid–liquid interfacial tension. Spreading coefficients were also estimated from the interfacial tension according to relation (1).

$$S_i = \gamma_{jk} - (\gamma_{ij} + \gamma_{ik}) \quad (1)$$

where γ_{jk} is the interfacial tension between the phases j and k.

2.3.2. Conductometry

The electrostatic interactions between Chi and GA in an aqueous solution were measured by conductometric titration. Conductivity measurements were performed using a CMD210 conductometer equipped with a CDC749 cell (Radiometer Copenhagen) at room temperature.

2.3.3. Zeta potential

The electrical charge measurements of the solutions and particles were performed using a Zetasizer 2000 (Malvern Instruments Ltd., Malvern, UK) at room temperature, with reproducibility being checked by performing three repeated measurements. The solutions were diluted with acetic acid solution (pH 3.6) ten times before being injected into the measurement cell.

2.3.4. Viscosity

The viscosity of each solution was determined by a viscosimeter Rheomat RM100 of type Taylor-Couette flow at 930 rpm during 40 s at room temperature.

2.3.5. Particle size analysis

Particle diameters were obtained with a laser-light blocking technique (AccusizerTM, model 770, Particle sizing systems, Santa Barbara, CA, and C770 software version 2.54). The particle size distribution was constructed one particle at a time, by comparing the detected pulse heights with standard calibration curve, obtained from a set of uniform particles of known diameter. All samples were diluted 100 times in acidic solution of de-ionized water before being analyzed. Measurements were performed in triplicate at room temperature. Data obtained were expressed as the mean particle diameter. All particle size measurements were repeated 3 times per sample and each sample was prepared in triplicate. The average values and standard deviations were calculated.

2.3.6. Morphology of the particles

The microscopic aspects of the particles were observed by both optical microscopy (Axioskos Zeiss) equipped with a camera (IVC 800 12 S) and scanning electron microscopy (Philips XL30 ESEM/EDAX- SAPPHIRE).

2.3.7. Infrared spectroscopy

The structure of the shell polymer was analyzed by FT-IR spectra. Samples were ground and mixed with KBr to make pellets. FTIR spectra in the absorbance mode were recorded using a Nicolet Nexus, connected to a PC, in which the number of scans was 128 and the resolution was 4 cm^{-1}.

3. Results and discussion

Microencapsulation was carried out by using a complex coacervation technique. The process includes two main steps, e.g. emulsification step which determines the size and the size distribution of the microcapsules; and the formation of the polymeric shell around the capsules. The emulsification step may be influenced at once by physical parameters such as apparatus configuration, stirring rate, volume ratio of the two phases, and by physicochemical properties such as interfacial tension, viscosities, densities and the chemical compositions of the two phases. The second step is governed by the ability of the two oppositely charged polyions to complex. The complexation depends on the charge density of both biopolymers related to the pH, the ionic strength, the total biopolymer concentration and on the ratio of the two biopolymers. Each step was keenly observed to understand their effects on the particle size and on the formation mechanism of the shell. Thus, to determine the optimal conditions for the synthesis of Chi-GA microcapsules containing miglyol solution, the study is based on (i) the determination of amount ratio of Chi to GA to yield optimal coacervation, the pH of coacervation; (ii) the influence of the stirring time and dispersed to continuous phase ratio on the emulsion stability and particle size distribution; and (iii) the shell formation predicted from the thermodynamic behavior of each phase and the cross-linking step.

3.1. Chi-GA interactions in solution

Attractive interactions between Chi and GA can lead to the precipitation of the both polymers when the mutual neutralization of anionic polysaccharides decreases the net charge and the hydrophilicity of the junction zones and also when it reduces the macromolecular backbone rigidity, which induces the phase separation of the system and therefore the complex coacervation (Espinosa-Andrews et al., 2010). These interactions, mostly induced by electrostatic attractions between oppositely charged biopolymers, induce the formation of complexes, which can be insoluble to form a two-phase system consisting of complex-rich and solvent-rich phases, also called associative separation. The formation of these complexes is closely related to the pH of the two solutions as well as the weight ratio of Chi-GA mixtures.

The variation of the conductivity of the various chitosan (1%, 2% and 3% w/v) and gum Arabic (1%, 2%, 3%, 5% and 10% w/v) solutions are depicted in Fig. 1. Conductivity is based on the movements of ions in solution, and since chitosan is a polyelectrolyte, at a higher concentration, a greater number of ions per unit volume of solution was present. PH adjustment of the chitosan solutions from the solubilization to pH 2 was realized with acetic acid solution and hydrochloric acid was used for pH below 2. Conductivities curves may be divided in three parts, in which firstly the conductivity values decreases between the pH of solubilization to pH ~4, secondly a plateau is reached between pH 4 to 2.8, and then the conductivities increases until pH 1.5. On the one hand, when chitosan dissolves in hydrochloric acid (pH less than 2), amino groups on chitosan chains bind free protons which involves an extended coil structure due to electrostatic repulsions. With the increase of concentration, more protons are bound, which leads to a decrease of the conductivity since the amount of free ions in the solution decreases. On the other hand, when chitosan dissolves in acetic acid solution, amino groups first dissociated H^+ from carboxylic acid molecules, which is illustrated by the slight decrease of conductivity values from solubilization pH to 4. From pH 3.6, the dissociated protons are completely bound, and with the concentration increase or pH decrease until 2, more chitosan chains interact with undissociated carboxylic acid molecules which induces an increase of the conductivity (Li, Song, Yang, & Fan, 2006). There, the presence of the inflexion point at pH 3.6 indicates the end of amino group protonation. Furthermore, Li et al. have proposed that the carboxylic acidic ions and hydrion move orderly along the complex formed from chitosan and carboxylic acid molecules and the increase of the chitosan concentration leads to more complex forms (Li et al., 2006). Gum Arabic is an anionic polysaccharide, and conductivity remains constant above the pK_a, when the carboxylic acid groups come close to this value, they release a proton and become negatively charged.

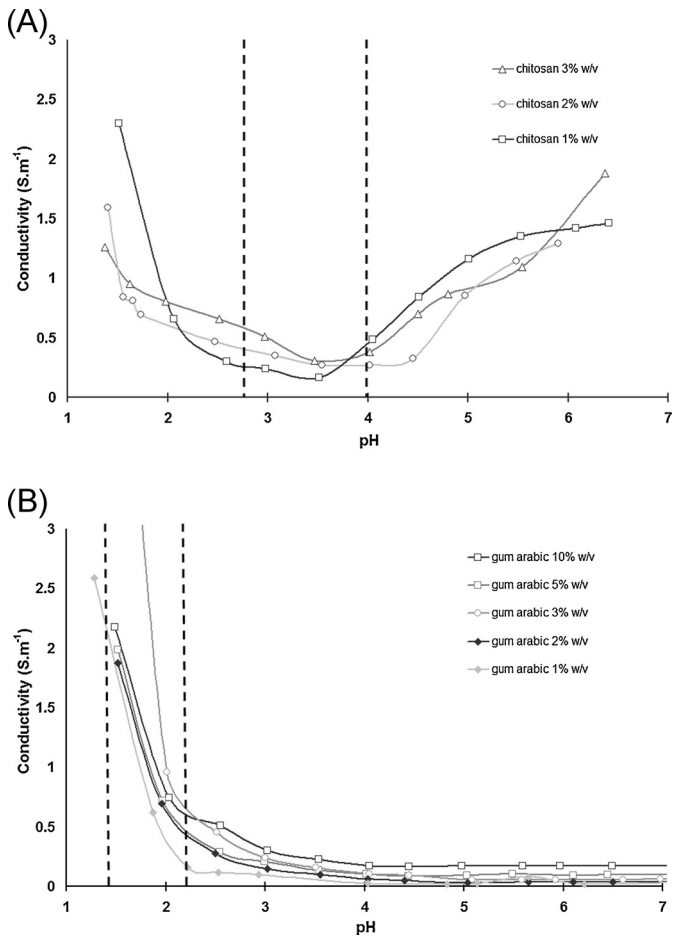

Fig. 1. Variation of conductivity of various amount of chitosan (A) and Arabic gum (B).

From the slope change of the conductivity, the pK_a of the acidic groups of the GA is between 1.8 and 2.2. Therefore, since gum Arabic is negatively charged above pH 2.2 and chitosan solutions have a maximum of charge in the range of 2.8–4, the pH of the solutions about 3.6 was considered as an optimum pH for interactions between the two solutions, independently of theirs concentrations.

Fig. 2 shows the ratio of conductivities of Chi/GA as a function of the biopolymers initial ratio ($R_{Chi/GA}$) in the solution at pH 3.6. Different weight ratios of chitosan to gum Arabic at different concentrations were prepared by mixing the appropriate quantities. Then, it was observed that the conductivity ratio increased proportionally with the increase of biopolymer ratio (slope about 4.2 for all the tested solutions), corresponding to a maximum of interactions between both polysaccharides since at this pH the ionized groups are mutually neutralized and lead to the formation of complex coacervation. Therefore, the maximum of coacervation occurs for 4 (or 5) g of gum Arabic per gram of chitosan. This result is close to those of Espinosa-Andrews, Baez-Gonzalez, Cruz-Sosa, and Vernon-Carter (2007) and Moschakis et al. (2010), who reported an initial ratio ($R_{GA/Chi}$) about 5 for a medium molecular weight chitosan.

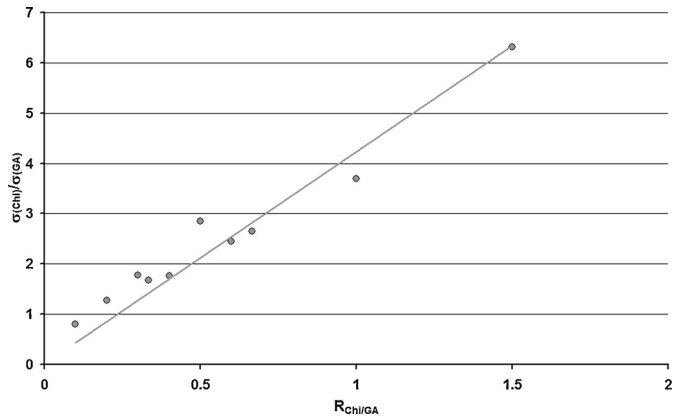

Fig. 2. Chitosan/Arabic gum conductivities ratio as a function of polymers ratio.

From these results, three kind of mixtures were monitored by measuring the electrokinetic properties and the coacervation yield at pH 3.6 (determined as the ratio of the recovered dried coacervated particles to the weight of both biopolymers introduced), i.e. mixture n°1 (50 mL of gum Arabic solution at 8% w/v and 50 mL of chitosan solution at 2% w/v); mixture n°2 (50 mL of gum Arabic solution at 10% w/v and 50 mL (+20 mL) of chitosan solution at 2%); and mixture n°3 (100 mL of gum Arabic at 5% w/v and 50 (+50) mL of chitosan solution at 2% w/v) (Fig. 3). All the mixtures show negative zeta potential, chitosan became positively charged at pH 3.6 and interacted with GA, negatively charged. The addition of chitosan solution led to a neutralization of the GA solutions. Thus, 40, 60 and 70 mL of chitosan at 2% w/v are required to neutralize the negative charge of GA solutions at 8% w/v (50 mL), 10% w/v (50 mL) and 5% w/v (100 mL), respectively; which corresponds to a $R_{chi/GA}$ value between 0.2 and 0.28. Furthermore, at pH 3.6, a coacervate yield of 74% was detected for the mixtures n°1 and n°2, and 84% for the mixture n°3.

The results of the zeta potential measurements were in good agreement with the $R_{Chi/GA}$ values determined previously at pH 3.6 from the conductivity measurements. It was also observed that in the mixtures stored at room temperature for several hours, the formed complexes of gum Arabic and chitosan remain in dispersion from the first mixture, whereas they form solid sediment that accumulate in the bottom of the flask for the two other mixtures. Therefore, for preparing good encapsulated material, it is important to maintain stirring during the whole process to avoid phase separation. Furthermore, the coacervated layer may be chemically cross-linked in order to keep it irreversible. According to the previous result, the mixture selected for the microencapsulation process is the mixture n°1, i.e. a gum Arabic solution at 8% w/v and a chitosan solution at 2% (w/v).

3.2. *Effects of phase volume ratio and stirring time on emulsion properties*

Particle formation during the homogenization depends on a stress balance between the turbulent forces tending to break up the droplet and the forces from interfacial tension holding a droplet together. The degree of a liquid droplet break-up is leaded by three forces, i.e. surface tension that tries to maintain the spherical shape, viscous and inertial forces attempt to deform the droplet. The droplet size is determined by a balance between the droplet break-up and the coalescence forces. These two factors are considered to be the most important phenomena determining the droplet size and size distribution in emulsification process. The effect of the volume ratio between the dispersed phase and the continuous phase is shown in Figs. 4 and 5. Emulsions of four ratios (0.05, 0.10, 0.15 and 0.20) were prepared by homogenization at 11,000 rpm using a rotor/stator apparatus during 5, 10, 15, 20, 25 and 30 min. In emulsion systems, the adsorption of gum Arabic at the oil-water interface allows steric hindrance preventing the droplets to come in closer contact. Moreover the gum being negatively charged above pH 2 allows electrostatic stabilizations of emulsions. As seen in Fig. 5, an identical equilibrium emulsion droplet size was reached in all cases after 15 min. Furthermore, the time duration to obtain a

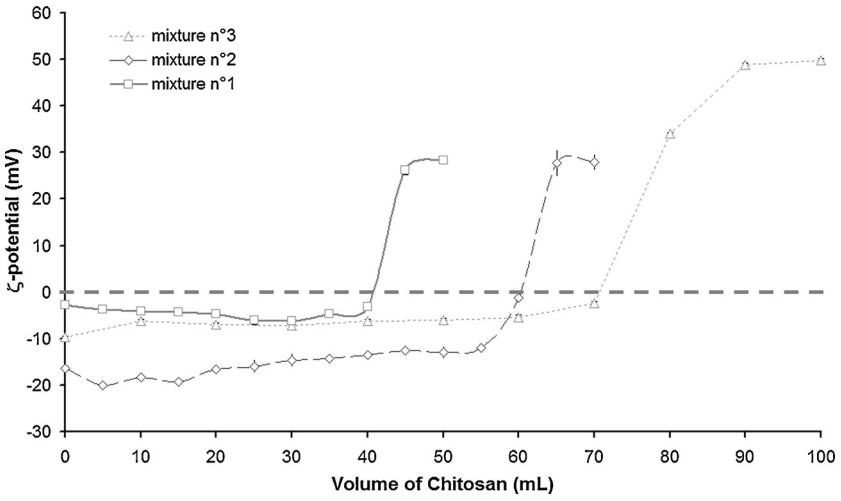

Fig. 3. Electrokinetic measurements of gum Arabic gum/chitosan mixture as a function of chitosan volume added.

narrow particle size distribution decreases with the increasing of the volume ratio. Particle mean diameter tends to decrease with the amount of oil volume introduced from 7.9 μm for a ratio volume of 0.05–1.27 for a *r* value of 0.2 (Fig. 4). After storage at room temperature, a creaming phenomenon of the droplet was observed after several hours, related to the difference in density between the two phases. The lower the volume ratio is, the faster the creaming rate is. The latter varies from 2 h for $r = 0.05$ and to 24 h for $r = 0.2$. After two days, all the solutions are separated in two phases, where the lower phase is a Miglyol microemulsion in the water formed by the satellite micro-droplets whereas the higher phase is mainly made up of larger Miglyol droplets in suspension in the aqueous phase. Emulsions composed of droplets in the micron-size range are not thermodynamically stable and there are various sources of instability ultimately leading to phase separation. Creaming of droplets can occur depending on the density difference between the dispersed and continuous phase and can be enhanced or restricted by flocculation. After 48 h, no variation of the mean droplet size was observed for low *r*, whereas for $r = 0.15$ and $r = 0.2$ coalescence has taken place. Furthermore, the size variation was also correlated to the viscosity of the solutions (Fig. 4). Thus, an increase of the viscosity allows to decrease the mean size of the particles. The above results indicate that the stability of the emulsion was significantly

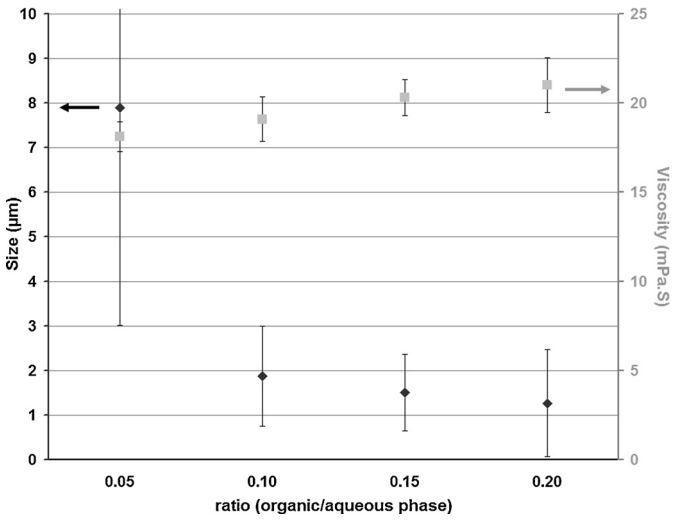

Fig. 4. Effect of organic/aqueous phase ratio on the mean diameter and viscosity of the solutions (stirring time = 15 min).

depended on the *r* value and the storage time, and therefore the optimum volume ratio chosen is 0.10 for the microencapsulation process and an emulsion time of 15 min at 11,000 rpm.

3.3. Shell microcapsule formation

Gum Arabic–chitosan microcapsules were prepared by complex coacervation. According to this method, the formation of microcapsules results from a surface phenomenon due to the interaction between both biopolymeric solutions at the oil in water interface. Gum Arabic used as emulsifier; is also dispersed in the continuous phase and contributes to the formation of coacervated particles which tend to deposit at the interface.

3.3.1. Mechanism of shell formation – functional group interactions

Adsorption of biopolymers and coacervated particles on the core phase is a key step in the microencapsulation process based on polymer phase separation phenomena, therefore the determination of the interfacial tensions between the dispersed and continuous phases as well as the calculation of the spreading coefficient were used to predict the final morphology of the final particles. Calculation of spreading coefficients, between the different interfaces present requires the knowledge of surface and interfacial tensions determined either from the measurement of contact angle or from the Wilhelmy's method. The resulting interfacial characteristics for the possible pairs are given in Table 2. The entrapment depends on the spreading behavior of the Miglyol and continuous phase on the GA-Chi coacervated particles surface. From these results, the interfacial tension between GA-Chi coacervated particles and miglyol is by 7.4 mN m^{-1} larger than the respective value for the pair GA-Chi coacervated particles/continuous phase. This reveals a larger affinity of the GA-Chi coacervated particles for the core phase than the continuous medium. Therefore, the calculated spreading coefficients between continuous phase, and Miglyol and coacervated particles were negative whereas it was positive for the continuous phase/Miglyol interface. The calculated work of adhesion reveals stronger interactions between GA-Chi coacervated microparticles and continuous phase than between GA-Chi coacervated and core solution. According to these calculations GA-Chi coacervated particles are suitable to entrap the core solution.

The FT-IR Spectra of Miglyol, used as dispersed phase, and gum Arabic–chitosan particles are presented in Fig. 6 to allow the identification of various core and shell microcapsules via known

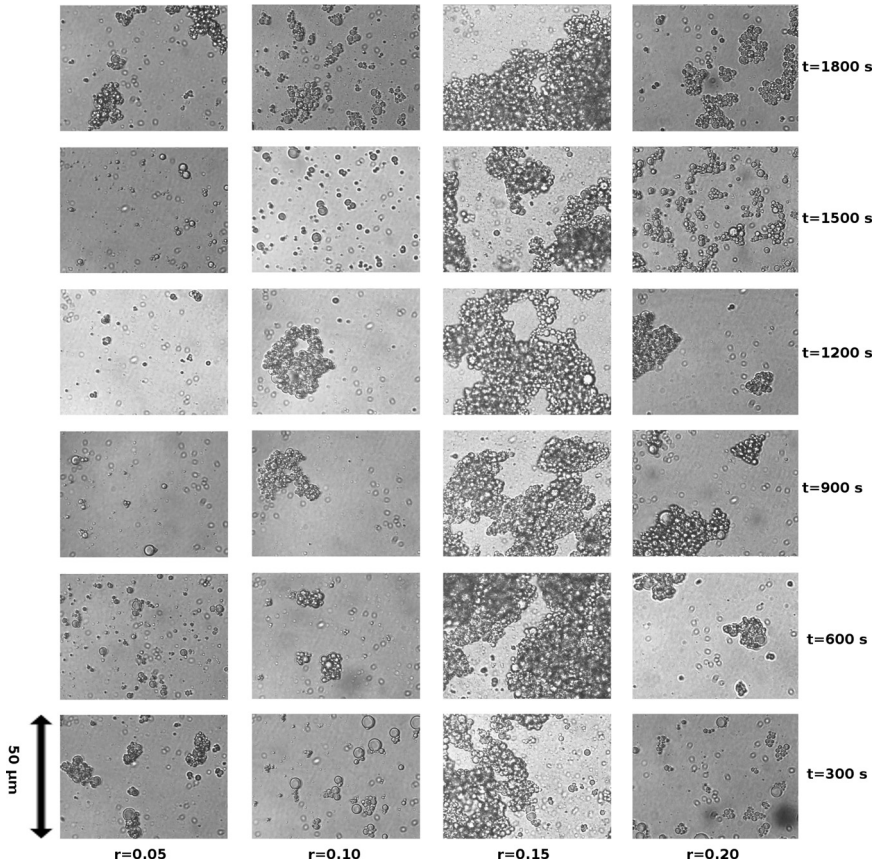

Fig. 5. Effects of organic/aqueous phase ratio on the properties of the emulsion.

characteristic wavenumbers. As seen in the figure, the spectrum (a) shows strong absorption bands at 2956, 2926 and 2855 cm^{-1} associated to the aliphatic C—H asymmetrical and symmetrical stretching vibration of the Miglyol. The in-plane rocking vibration of the CH_2 groups is observed at 720 cm^{-1}, and C—H bending vibration in CH_2 is found at 1465 cm^{-1} and 1378 cm^{-1}. Characteristic band of the ester carbonyl functional group of the triglycerides is also observed at 1743 cm^{-1}. The C—O stretching appeared at 1230, 1170 and 1064 cm^{-1}, whereas the stretching vibration of the C—O ester groups was detected at 1108 cm^{-1}. The gum Arabic–chitosan particles spectrum (Fig. 6-S7-1 (before the crosslinking stage)) was analyzed in its solid state. This spectrum showed characteristics broad band at 3348 cm^{-1} concerned with —OH groups of both biopolymers and overlapped the stretching band of —NH. Furthermore, this broad band underlines hydrogen bonding involved in the interaction between GA and Chi. The C—H stretching vibration was also observed at 2926 cm^{-1}, the small shoulder at 1660 cm^{-1} a characteristic amide band corresponding to the C=O vibration of the acetylated amino group indicating the high degree of deacetylation of the chitosan. The main characteristic bands of chitosan appeared at 1604 cm^{-1} for the —NH angular deformation and 1150–1040 cm^{-1} for the —C—O—C— linkage in the glycosidic structure. Furthermore, the absence of the carboxylic acid (—COOH) moities at 1255 cm^{-1}, shows that all the acid groups interacted with the $-NH_3^+$ of the chitosan. All of the characteristic peaks for Miglyol and gum Arabic–chitosan coacervates can be clearly distinguished in the spectra of the microcapsule samples, which verifies that the dispersed phase has been successfully encapsulated by complex coacervation.

Fig. 7 shows zeta potential variation during the miglyol encapsulation at various process stages. It can be observed that the emulsion has a low potential zeta about −20 mV, during the coacervation step, zeta potential of the solutions increases to −10 mV with the addition of 60 mL of chitosan solution and reaches positive values for higher volumes added (synthesis S6). When chitosan formed the outermost layer, a net positive surface charge due to excess chitosan was observed and the ζ-value is close to the chitosan solution one. Nevertheless, formed particles are not stable and collapse to be embedded in a gel phase (Fig. 8B). These results suggest that high volume of chitosan lead to the flocculation of the system, through the adsorption of chitosan chains on the surface of more than one negatively charged droplet (Klinkesom & Namatsila, 2009). Therefore, a cross-linking step is required to obtain solid and individual particles. Furthermore, it was also noticed that the amount of chitosan to neutralize the gum Arabic emulsion was lower than this previously established, due to the adsorption of gum Arabic chains onto the droplet surface.

3.3.2. *Influence of NaTPP as a cross-linking agent*

Chitosan, a strong cationic polyelectrolyte can interact through electrostatic interactions with a multivalent anionic molecule such as NaTPP to form an intermolecular complex. NaTPP dissolved in water dissociate to give phosphoric acid, the cross-linking of chitosan depends on the availability of the cationic sites of Chi and the presence of negative charges of NaTPP. To investigate the effect of crosslinking agent; the various stages of particle formation (sample S7) were monitored by Infrared Spectroscopy, and zeta potential measurements for all the samples listed in Table 1.

The FTIR observations (Fig. 6) show characteristic bands at 1222 cm^{-1} assigned to P—O stretching, 1157 cm^{-1} for the stretching vibration of the PO_2 groups, 1105 and 894 cm^{-1} attributed to the stretching vibration of the PO_3 groups and P—O—P asymmetric stretching, respectively. The increase of the intensity of the peak in the range of 1150–1160 cm^{-1} indicated the increase of

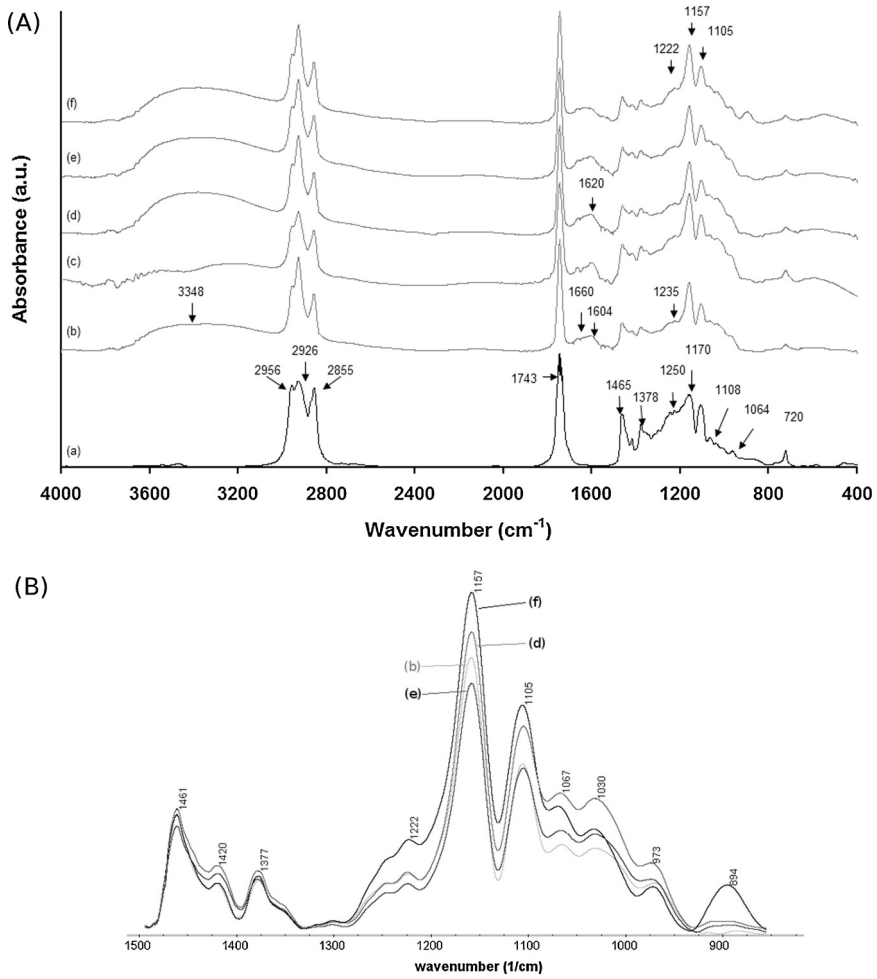

Fig. 6. FTIR spectra of core phase (a), GA-Chi coacervated particles (b (S7-1)), TPP crosslinked GA-Chi particles (c–5 mL NaTPP; d-(S7-2); e-(S7-3); f-(S7)). B–Zoom of the 1500–850 cm^{-1} area.

bound NaTPP ions (Fig. 6B, spectra b, d & f). Thus, it is clearly observed that the intensity of the P═O absorbance at 1222 cm^{-1} (and 1250 cm^{-1}) of the crosslinked particles increases with the NaTPP volume added in the solution, suggesting an increase of the crosslinking degree. Therefore, from the spectral analysis, it can be observed that the crosslinking was effective through ionic interaction among negatively charged P—-O^- moities of TPP and NH_3^+ of chitosan. This phenomenon was further confirmed by surface charge results (Fig. 7). Furthermore, from the spectrum e (sample S7-3), it can be also observed that further addition of chitosan

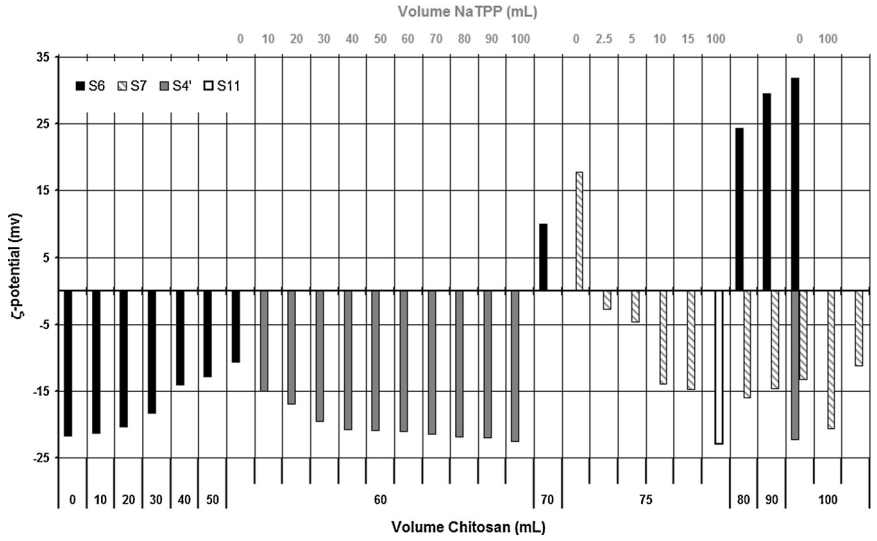

Fig. 7. Zeta potential variations of particles from syntheses 4, 6, 7 and 11 at various process steps according to the chitosan and NaTPP volumes added.

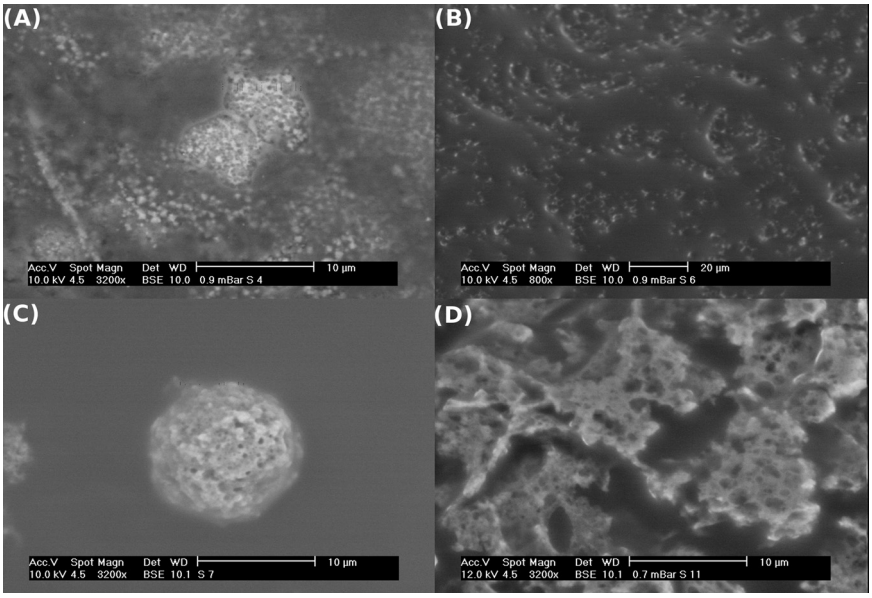

Fig. 8. SEM micrographs of particles from syntheses labeled S4 (A), S6 (B), S7 (C) and S11 (D).

Table 1
Formulation of gum arabic–chitosan microcapsules. Influence of the crosslinking steps on the loading content and encapsulation yield.

Sample code	Coacervation step	Crosslinking steps			Zeta potential	Encapsulation yield[a]	Loading content[b]
	Chitosan (2% w/v) (mL)	Step n°1 NaTPP (2% w/v) (mL)	Step n°2 Chitosan (2% w/v) (mL)	Step n°3 NaTPP (2% w/v) (mL)	(mV)	(%)	(%)
S4	60	100	40		−22.3 (±0.9)	91.3	63.1
S6	100	–	–	–	31.9 (±1.1)	–	67.4
S7-1	75	–	–	–	17.8 (±0.8)	–	–
S7-2	75	15	–	–	−14.7 (±0.5)	–	–
S7-3	75	15	25	–	−13.3 (±0.7)	–	–
S7	75	15	25	85	−20.6 (±0.2)	97.0	59.0
S11	75	100	–	–		95.2	57.6

[a] The encapsulation yield was calculated according to the following equation: Encapsulation yield = [(Dry weight of microcapsules)/(Total weight of chitosan, gum Arabic and core solution in the emulsion)] × 100.
[b] The loading content was calculated from: [(total amount of core solution − free core solution)/(total amount of core solution)] × 100.

Table 2
Characteristics of different interfaces present in the microencapsulation medium in the microencapsulation process.

Interfaces	Interfacial tension (mN m^{-1}) γ_{sl}	Work of adhesion (mN m^{-1}) W_a	Spreading coefficient (mN m^{-1}) S_i
Miglyol/GA-Chi coacervates	7.4[a1]	15.9	−22.9
Continuous phase/GA-Chi coacervates	1.3[a2]	22.1	−10.7
Continuous phase/miglyol	16.8	54.0	8.0

[a] Calculated from the mean contact angle using Young's equation: $\gamma_{sv} = \gamma_{sl} + \gamma_{lv} \cos\theta_i$, with $\theta_1 = 23.2°$ and $\theta_2 = 65.6°$.

results in the decrease of the intensity at 1222 cm^{-1}, which may be related to an uncompleted interaction between chitosan and NaTPP. Higher chitosan concentrations lead to more unneutralized $-NH_3^+$ on the surface of complexes.

A significant decrease of zeta potential value of the particles was observed after the addition of 40 mL of NaTPP solution, before the neutralization of the solution by chitosan addition, which remained constant thereafter to reach the value of the NaTPP one, in the case of the S4 synthesis. Furthermore, it was also noticed that the deposition of another layer with chitosan was not possible. An excess at the particle surface may involve agglomeration due to the crosslinkage between the particles (Fig. 8A and D). The incorporation of NaTPP in a single step after neutralization of the GA emulsion has the same influence (synthesis labeled S11). Therefore, 15 mL of NaTPP solution was added to switch from positive to negative zeta potential values, in the synthesis S7. When 25 mL of chitosan was further added to form the outermost layer, the ζ-value was found increase, due to the interaction of TPP negatively charged and chitosan, which is proved by the deposition of the cationic biopolymer. This sample was also treated with 100 mL of NaTPP to solidify the outer shell. It was observed that the zeta potential increased from −20.6 mV before storage to −11.2 mV after 12 h, corresponding to the diffusion of the anionic charge in the chitosan network (Fig. 7). The SEM micrograph (Fig. 8C) shows the presence of individual particle with a rough surface layer. This shell was also composed from smaller coacervated particles formed in the continuous medium which cover the core.

4. Conclusion

Formation of gum Arabic–chitosan microcapsules with mean diameter between 5 and 10 μm was successfully achieved by

complex coacervation of gum Arabic and chitosan and ionic crosslinking steps by NaTPP, as predicted from the thermodynamical approach. In this study, process parameters affecting either the formation of a stable emulsion or shell formation step during the microencapsulation process were also investigated. It was found from particle size analysis that the optimum emulsion conditions were obtained with a phase volume ratio of 0.15, the stirring rate and time were adjusted to allow the formation of microcapsules in the range of 5–10 μm. Furthermore, it was also established that the preparation of capsules was performed at pH 3.6 to obtain the maximum of electrostatic interaction between both biopolymers for an initial ratio ($R_{Chi/GA}$) of 0.25 to obtain high encapsulation yield.

References

Alonso, D., Gimeno, M., Sepúlveda-Sánchez, J. D., & Shirai, K. (2010). Chitosan-based microcapsules containing grapefruit seed extract grafted onto cellulose fibers by a non-toxic procedure. *Carbohydrate Research*, *345*(6), 854–859.

Argin-Soysal, S., Kofinas, P., & Lo, Y. M. (2009). Effect of complexation conditions on xanthan–chitosan polyelectrolyte complex gels. *Food Hydrocolloids*, *23*(1), 202–209.

Avadi, M. R., Sadeghi, A. M. M., Mohammadpour, N., Abedin, S., Atyabi, F., Dinarvand, R., & Rafiee-Tehrani, M. (2010). Preparation and characterization of insulin nanoparticles using chitosan and Arabic gum with ionic gelation method. *Nanomedicine: Nanotechnology, Biology, and Medicine*, *6*(1), 58–63.

Bansode, S. S., Banarjee, S. K., Gaikwad, D. D., Jadhav, S. L., & Thorat, R. M. (2010). Microencapsulation: A review. *International Journal of Pharmaceutical Sciences Review and Research*, *1*(2), 38–43.

Bendkowska, W. (2006). Intelligent textiles with PCMs. In H. R. Mattila (Ed.), *Intelligent textiles and clothing* (pp. 34–62). Cambridge: Woodhead Publishing Ltd.

Boh, B., & Sumiga, B. (2008). Microencapsulation technology and its applications in building construction materials. *Materials and Geoenvironment*, *55*(3), 329–344.

Bungenberg de Jong, H. G., & Kruyt, H. R. (1929). Coacervation (partial miscibility in colloid systems). *Proceedings of the Koninklijke Nederlandse Akademie der Wetenschappen*, *32*, 849–856.

Chatterjee, S., Salaün, F., Campagne, C., Vaupre, S., & Beirão, A. (2012). Preparation of microcapsules with multi-layers structure stabilized by chitosan and sodium dodecyl sulfate. *Carbohydrate Polymers*, *90*(2), 967–975.

Chávarri, M., Marañón, I., Ares, R., Ibáñez, F. C., Marzo, F., & Villarán, M. d. C. (2010). Microencapsulation of a probiotic and prebiotic in alginate-chitosan capsules improves survival in simulated gastro-intestinal conditions. *International Journal of Food Microbiology*, *142*(1–2), 185–189.

Coelho, S., Moreno-Flores, S., Toca-Herrera, J. L., Coelho, M. A. N., Carmo Pereira, M., & Rocha, S. (2011). Nanostructure of polysaccharide complexes. *Journal of Colloid and Interface Science*, *363*(2), 450–455.

de Kruif, C. G., Weinbreck, F., & de Vries, R. (2004). Complex coacervation of proteins and anionic polysaccharides. *Current Opinion in Colloid and Interface Science*, *9*(5), 340–349.

Deveci, S., & Basal, G. (2009). Preparation of PCM microcapsules by complex coacervation of silk fibroin and chitosan. *Colloid and Polymer Science*, *287*(12), 1455–1467.

Elmer, C., Karaca, A. C., Low, N. H., & Nickerson, M. T. (2011). Complex coacervation in pea protein isolate–chitosan mixtures. *Food Research International*, *44*(5), 1441–1446.

Espinosa-Andrews, H., Baez-Gonzalez, J. G., Cruz-Sosa, F., & Vernon-Carter, E. J. (2007). Gum Arabic - chitosan complex coacervation. *Biomacromolecules*, *8*(4), 1313–1318.

Espinosa-Andrews, H., Sandoval-Castilla, O., Vázquez-Torres, H., Vernon-Carter, E. J., & Lobato-Calleros, C. (2010). Determination of the gum Arabic–chitosan interactions by Fourier Transform Infrared Spectroscopy and characterization of the microstructure and rheological features of their coacervates. *Carbohydrate Polymers*, *79*(3), 541–546.

Fernandes, S. C., de Oliveira, I. R. W. Z., Fatibello-Filho, O., Spinelli, A., & Vieira, I. C. (2008). Biosensor based on laccase immobilized on microspheres of chitosan crosslinked with tripolyphosphate. *Sensors and Actuators B: Chemical*, *133*(1), 202–207.

Garud, A., & Garud, N. (2010). Preparation and evaluation of chitosan microcapsules of metronidazole using tripolyphosphate cross-linking method. *The Dhaka University Journal of Pharmaceutical Sciences*, *9*(2), 125–130.

Gómez-Burgaz, M., García-Ochoa, B., & Torrado-Santiago, S. (2008). Chitosan–carboxymethylcellulose interpolymer complexes for gastric-specific delivery of clarithromycin. *International Journal of Pharmaceutics*, *359*(1–2), 135–143.

Hsieh, W.-C., Chang, C.-P., & Gao, Y.-L. (2006). Controlled release properties of Chitosan encapsulated volatile Citronella Oil microcapsules by thermal treatments. *Colloids and Surfaces B: Biointerfaces*, *53*, 209–214.

Huang, G.-Q., Sun, Y.-T., Xiao, J.-X., & Yang, J. (2012). Complex coacervation of soybean protein isolate and chitosan. *Food Chemistry*, *135*(2), 534–539.

Hussain, M. R., & Maji, T. K. (2008). Preparation of genipin cross-linked chitosan-gelatin microcapsules for encapsulation of Zanthoxylum limonella oil (ZLO) using salting out method. *Journal of Microencapsulation*, *4*, 1–7.

Klinkesom, U., & Namatsila, Y. (2009). Influence of chitosan and NaCl on physicochemical properties of low-acid tuna oil in water emulsions stabilized by non-ionic surfactant. *Food Hydrocolloids*, *23*(5), 1374–1380.

Kumbar, S. G., Kulkarnu, A. R., & Aminabhavi, M. (2002). Crosslinked chitosan microspheres for encapsulation of diclofenac sodium: Effect of crosslinking agent. *Journal of Microencapsulation*, *19*, 173–180.

Lee, A.-C., & Hong, Y.-H. (2009). Coacervate formation of α-lactalbumin–chitosan and β-lactoglobulin–chitosan complexes. *Food Research International*, *42*(5–6), 733–738.

Li, J., & Huang, Q. (2012). Rheological properties of chitosan–tripolyphosphate complexes: From suspensions to microgels. *Carbohydrate Polymers*, *87*(2), 1670–1677.

Li, Q.-X., Song, B.-Z., Yang, Z.-Q., & Fan, H.-L. (2006). Electrolytic conductivity behaviors and solution conformations of chitosan in different acid solutions. *Carbohydrate Polymers*, *63*(2), 272–282.

Mi, F.-L., Shyu, S.-S., Lee, S.-T., & Wong, T.-B. (1999). Kinetic study of chitosan-tripolyphosphate complex reaction and acid-resistive properties of the chitosan-tripolyphosphate gel beads prepared by in-liquid curing method. *Journal of Polymer Science Part B: Polymer Physics*, *37*(14), 1551–1564.

Morris, G. A., Castile, J., Smith, A., Adams, G. G., & Harding, S. E. (2011). The effect of prolonged storage at different temperatures on the particle size distribution of tripolyphosphate (TPP)–chitosan nanoparticles. *Carbohydrate Polymers*, *84*(4), 1430–1434.

Moschakis, T., Murray, B. S., & Biliaderis, C. G. (2010). Modifications in stability and structure of whey protein-coated o/w emulsions by interacting chitosan and gum Arabic mixed dispersions. *Food Hydrocolloids*, *24*(1), 8–17.

Nelson, G. (2002). Application of microencapsulation in textiles. *International Journal of Pharmaceutics*, *242*(1–2), 55–62.

Pedro, A. S., Cabral-Albuquerque, E., Ferreira, D., & Sarmento, B. (2009). Chitosan: An option for development of essential oil delivery systems for oral cavity care? *Carbohydrate Polymers*, *76*(4), 501–508.

Salaün, F., Creach, G., Rault, F., & Almeras, X. (2013). Thermo-physical properties of polypropylene fibers containing a microencapsulated flame retardant. *Polymers for Advanced Technologies*, *24*(2), 236–248.

Salaün, F., Devaux, E., Bourbigot, S., & Rumeau, P. (2010). Thermoregulating response of cotton fabric containing microencapsulated phase change materials. *Thermochimica Acta*, *506*(1-2), 82–93.

Shao, Y., Zhu, B., Li, J., Liu, X., Tan, X., & Yang, X. (2009). Novel chitosan microsphere-templated microcapsules suitable for spontaneous loading of heparin. *Materials Science and Engineering: C*, *29*(3), 936–941.

Wu, M.-Y., Ning Chen, Liu, L.-K., Hua Yuan, Li, Q.-L., & Chen, S.-H. (2009). Chitosan/alginate multilayer scaffold encapsulating bone marrow stromal cells in situ on titanium. *Journal of Bioactive and Compatible Polymers*, *24*(4), 301–315.

Yadav, S. K., Suresh, A. K., & Khilar, K. C. (1990). Microencapsulation in polyurea shell by interfacial polycondensation. *AIChE Journal*, *36*(3), 431–438.

Yuan, Y., Chesnutt, B. M., Utturkar, G., Haggard, W. O., Yang, Y., Ong, J. L., & Bumgardner, J. D. (2007). The effect of cross-linking of chitosan microspheres with genipin on protein release. *Carbohydrate Polymers*, *68*(3), 561–567.